

Ultrathin ZrO₂ films on Si-rich SiC(0001)-(3 × 3): Growth and thermal stability

P.G. Karlsson^a, L.I. Johansson^b, J.H. Richter^a, C. Virojanadara^b, J. Blomquist^c,
P. Uvdal^c, A. Sandell^{a,*}

^a Department of Physics, Uppsala University, Box 530, SE-75121 Uppsala, Sweden

^b Department of Physics and Measurement Technology, Linköping University, SE-58183 Lund, Sweden

^c Chemical Physics, Lund University, Box 118, SE-22100 Lund, Sweden

Received 5 February 2007; accepted for publication 4 April 2007

Available online 11 April 2007

Abstract

The growth and thermal stability of ultrathin ZrO₂ films on the Si-rich SiC(0001)-(3 × 3) surface have been explored using photoelectron spectroscopy (PES) and X-ray absorption spectroscopy (XAS). The films were grown *in situ* by chemical vapor deposition using the zirconium tetra *tert*-butoxide (ZTB) precursor. The O 1s XAS results show that growth at 400 °C yields tetragonal ZrO₂. An interface is formed between the ZrO₂ film and the SiC substrate. The interface contains Si in several chemically different states. This gives evidence for an interface that is much more complex than that formed upon oxidation with O₂. Si in a 4+ oxidation state is detected in the near surface region. This shows that intermixing of SiO₂ and ZrO₂ occurs, possibly under the formation of silicate. The alignment of the ZrO₂ and SiC band edges is discussed based on core level and valence PES spectra. Subsequent annealing of a deposited film was performed in order to study the thermal stability of the system. Annealing to 800 °C does not lead to decomposition of the tetragonal ZrO₂ (t-ZrO₂) but changes are observed within the interface region. After annealing to 1000 °C a laterally heterogeneous layer has formed. The decomposition of the film leads to regions with t-ZrO₂ remnants, metallic Zr silicide and Si aggregates.

© 2007 Elsevier B.V. All rights reserved.

Keywords: Zirconium dioxide; Silicon carbide; Chemical vapor deposition; Semiconductor–insulator interfaces; Synchrotron radiation photoelectron spectroscopy; X-ray absorption spectroscopy

1. Introduction

Silicon carbide is a material suitable for high temperature, high power, high voltage and high frequency devices and sensors. Substantial efforts have been made in order to integrate SiC in MOSFET technology [1–3]. This work commonly entails the formation of a gate-insulating SiO₂ layer on top of the SiC substrate. The electronic properties are critically dependent on the interface properties. Photoelectron spectroscopy (PES) is a very useful tool to obtain

information on interface states and there are consequently a number of PES studies of the SiO₂/SiC interface [4–8].

Less attention has been paid to the deposition of a dissimilar oxide on SiC. An important set back for the use of SiO₂/SiC in SiC based MOS devices is the formation of electronically active interface states [2,3]. A high density of interface trap states near the conduction band limits the channel mobility. The use of an alternative oxide as gate insulator may be a way to circumvent this problem. The Al₂O₃/6H-SiC interface formed by atomic layer deposition shows for example a significantly reduced density of interface states [9].

ZrO₂ is an oxide with many attractive properties such as high thermal stability, low thermal conductivity and high dielectric constant. Pure and modified ZrO₂ is used for

* Corresponding author.

E-mail address: anders.sandell@fysik.uu.se (A. Sandell).

example as thermal barrier coating on gas turbine blades [10] and it is considered as a gate oxide material in Si based MOSFETs [11]. It has been demonstrated that MOS devices fabricated using ZrO_2 as dielectric show promise [12,13].

From the above follows that the combination of the two compounds SiC and ZrO_2 can be most useful for devices and materials that need to function at high temperatures. For example, ZrO_2 coated SiC is used as catalyst support and in turbine parts [14,15]. ZrO_2 may also prove to be an alternative as gate oxide in SiC based MOSFET devices. Consequently, a careful characterization of the ZrO_2/SiC system is well motivated.

The preparation of a well-defined substrate surface greatly facilitates the realization of a good oxide/SiC interface. The Si-rich SiC(0001)-(3 × 3) surface reconstruction is well defined and characterized in detail [4–8,16–20]. It is prepared by Si deposition at elevated temperature followed by additional annealing at higher temperature. From STM and LEED holography data a structural model has been derived in which the (3 × 3) surface is composed of Si-adatoms, Si trimers and a Si adlayer on top of the outermost Si–C bilayer [19,20]. Recent photoemission results reveal the presence of three surface components in the Si 2p spectrum, consistent with the structure model [8]. Extensive oxidation of the Si-rich (3 × 3) surface using O_2 at 800 °C results in complete oxidation of the surface Si atoms [7,8]. Only one suboxide, Si^{1+} , is observed besides the Si^{4+} species of fully developed SiO_2 [7,8].

In this paper, we present an investigation of the growth and thermal stability of ultrathin ZrO_2 on the Si-rich SiC(0001)-(3 × 3). The growth is undertaken by chemical vapor deposition under ultrahigh vacuum conditions. The growth is characterized in a stepwise fashion by employing synchrotron radiation excited photoelectron spectroscopy (PES) and X-ray absorption spectroscopy (XAS). Subsequent annealing of the deposited film was performed in order to study the thermal stability of the system.

2. Experimental

The spectra were recorded at beamline D1011 at the Swedish National Synchrotron Radiation Facility MAX-II [21]. The end station comprises a Scienta 200 mm radius hemispherical electron energy analyzer for PES measurements and a multichannel plate for recording of XAS spectra by collection of Auger electrons. The base pressure was in the low 10^{-10} mbar or better. The sample holder was made of tantalum and was etched in HCl prior to mounting. The tantalum clips holding the sample were annealed in vacuum. The PES spectra were all recorded at normal emission and the binding energy (BE) scales are referenced to the Fermi level of a sample holder clip. The intensity of each PES spectrum has been normalized to the current in the synchrotron storage ring. The intensity of a spectral component is defined as the integrated line profile. The relative magnification of each spectrum is given in the figures.

Upon new injection of the storage ring spectra have been re-measured. The XAS spectra were calibrated by using first- and second-order light from the monochromator.

The investigations were carried out on an n-doped 8° off cut 4H-SiC(0001) sample on which a (3 × 3) surface reconstruction was prepared before the ZrO_2 deposition. The (3 × 3) surface reconstruction was prepared the common way by Si deposition at a substrate temperature of ~800 °C and subsequent annealing to ~1000 °C. This resulted in a well-ordered (3 × 3) surface as confirmed by low energy electron diffraction (LEED).

ZrO_2 was deposited at a sample temperature of 400 °C using zirconium tetra *tert*-butoxide (ZTB) as single source precursor. The ZTB liquid was purified by multiple freeze–pump–thaw cycles. The sample was exposed to ZTB via a dosing tube (10 mm in diameter) positioned a few mm from the sample surface. The high vacuum parts of the ZTB dosing system were thoroughly baked out and subsequently passivated by exposing them to ZTB. The pressure during deposition was 2×10^{-8} mbar, read as the background pressure in the chamber.

The film was grown in intervals between which measurements were performed. After a total exposure time of 1700 s the resulting film was subsequently annealed to higher temperatures: 600, 800 and 1000 °C. The duration of each annealing was 60 s and the pressure never exceeded 3×10^{-9} mbar during annealing. The changes observed after annealing to 600 °C were negligible.

3. Results and discussion

3.1. Film growth

3.1.1. Overlayer thickness and local structure

Fig. 1 shows the film thickness as function of ZTB exposure time. The film thickness is estimated from the attenuation of the component in the Si 2p PES signal attributed

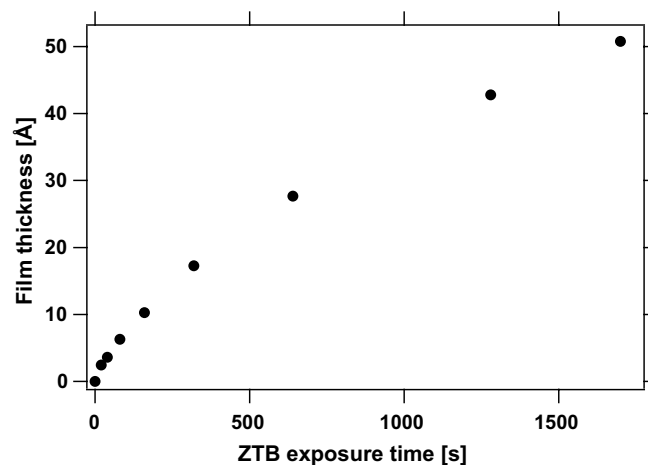


Fig. 1. Estimated film thickness as a function of deposition time. Growth conditions: Sample temperature 400 °C and ZTB background pressure 2×10^{-8} mbar. The film thickness is estimated from the attenuation of the component in the Si 2p PES signal attributed to SiC bulk.

to SiC bulk. The Si 2p intensities were obtained from spectra measured using the photon energy 758 eV. The mean free path (λ) is set to 20 Å. The choice of λ is supported by a comparison made for ZrO₂ on Si(100), where the film thickness estimated from an independent X-ray reflectivity measurement is in good agreement with that obtained by PES using $\lambda = 20$ Å at 758 eV photon energy. Note that zero film thickness is defined for the Si-rich SiC(0001) surface, which actually has silicon layers on top of the SiC substrate. Fig. 1 shows that the growth series encompasses thicknesses ranging from 4 Å to 51 Å. Given that the lattice parameters for t-ZrO₂ are $a = b = 3.6$ Å and $c = 5.2$ Å [22], the films range from approximately monolayer thickness up to an equivalent of about 10 t-ZrO₂ layers. However, this estimate is rather crude since the formation of an extended interface must be taken into account, cf. below.

Selected O 1s XAS spectra are presented in Fig. 2. The spectral structures become sharper for each deposition step, indicating that the ZrO₂ overlayer becomes increasingly ordered, i.e. crystalline. The spectrum measured for the 51 Å thick film is similar to that of a thick film on Si(100). Since the spectrum for the ZrO₂/Si(100) system is typical for tetragonal ZrO₂ it can be concluded that the tetragonal phase also forms at sufficient film thickness on SiC(0001)-(3 × 3) at 400 °C [23]. In contrast, the signature of t-ZrO₂ is not as pronounced in the O 1s XAS spectrum at a film thickness of 28 Å. This is most clearly seen by observing the differences in the photon energy region 542–545 eV. The film thickness dependence of the O 1s XAS spectrum is similar to that reported for film growth on Si(111)-(7 × 7) but different from film growth on

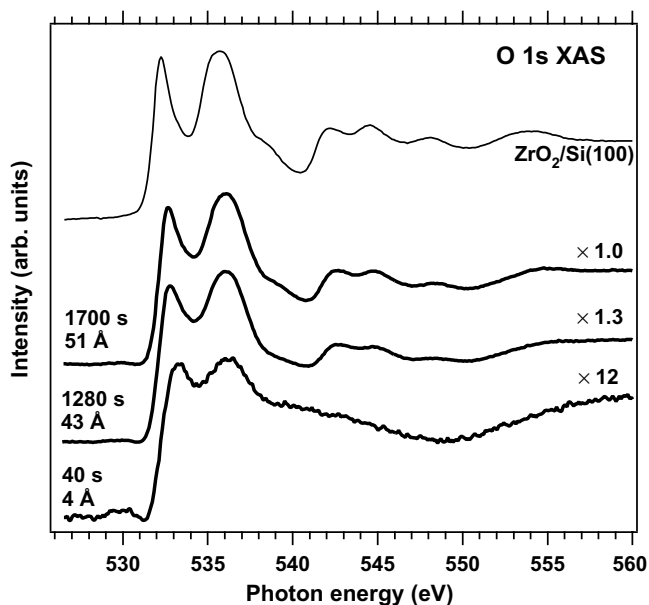


Fig. 2. O 1s XAS spectra for selected deposition steps. The photon energy resolution is 150 meV. The structures become sharper for each deposition step, indicating that the ZrO₂ overlayer becomes increasingly crystalline. The spectrum measured for the 51 Å thick film is similar to that of tetragonal ZrO₂ [23].

Si(100)-(2 × 1) where the fingerprint of crystalline ZrO₂ is observed at an earlier stage [23]. The similarity to Si(111)-(7 × 7) is not unexpected given that the Si overlayer on SiC(0001) and the Si(111) surface both have hexagonal symmetries. Another property that can be important for the geometric properties of the ZrO₂ film is the number of dangling bonds per surface atom [24]. The Si overlayer on SiC(0001) and the Si(111) surface both have one dangling bond per surface atom while the Si(100) surface has two dangling bonds per surface atom. It has been argued that two dangling bonds are more favorable for epitaxial ZrO₂ growth [24]. This is consistent with the observation of a delayed formation of crystalline ZrO₂ on Si-rich SiC(0001)-(3 × 3) and Si(111)-(7 × 7) as compared to growth on Si(100)-(2 × 1). However, it is most likely that also the presence of hydrocarbon fragments from the ZTB molecules strongly influence the geometric properties of the film at the initial stages of growth.

3.1.2. Photoemission of core levels

The Zr 3d PES spectra measured for 4 Å and 51 Å thick films are presented in Fig. 3. It is found that each of all Zr 3d spectra in the growth series can be described by one

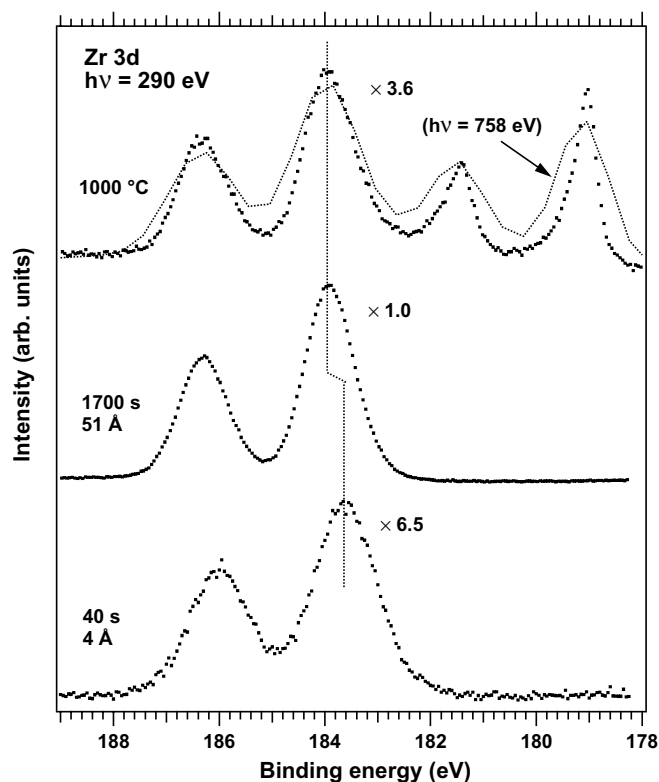


Fig. 3. Zr 3d PES spectra for selected situations. The total energy resolutions are 150 meV (290 eV photon energy) and 650 meV (758 eV photon energy). Each of all Zr 3d spectra in the growth series can be described by one spin-orbit pair attributed to Zr⁴⁺ (bottom and middle spectra). Upon subsequent annealing to 1000 °C a new additional component having an asymmetric line shape has appeared (top spectrum, large dots). The spectrum does not change dramatically when changing the surface sensitivity of the measurement (top spectrum, small dots).

spin–orbit pair. The Zr $3d_{5/2}$ BE is 183.6–183.9 eV, with the lower values found for thinner films. This BE range motivates an assignment to Zr^{4+} species [23]. Introduction of reduced species, which should be shifted at least -1 eV from the Zr^{4+} component [25], cannot be motivated. A broadening of the peaks for thinner films is furthermore observed. This can be related to e.g. an increased inhomogeneity for the situations where the film is likely to have a less defined stoichiometry and geometric structure.

The corresponding O 1s PES spectra (not shown) reveal only one component at about 531.7 eV BE throughout the growth series. The O 1s binding energies previously reported for ultrathin SiO_x on Si [26,27] and $ZrO_2/ZrSi_xO_y$ on Si [23,28] are similar to within 0.5 eV. Since the FWHM of the O 1s line is typically at least 1 eV, the small difference in BE could at most give rise to a broadening and not to two well-resolved peaks. The information gained from the O 1s spectra is thus limited with respect to the chemistry involved in the growth and interface formation. However, the O 1s BE is useful for a determination of the location of the conduction band edge for ZrO_2 as discussed below.

The C 1s PES spectra are presented in Fig. 4a. For the Si-rich $SiC(0001)-(3 \times 3)$ surface there is one symmetric peak at 283.0 eV BE attributed to SiC bulk. Upon ZTB exposure the SiC bulk peak is shifted, most probably because of changes in the band bending. After the first depo-

sition (4 \AA) the relative shift in BE amounts to $+0.34$ eV. The BE remains at a constant value up to 28 \AA . For thicker films there is an additional shift of about 0.15 eV. It cannot be excluded that sample charging contributes to this effect.

An additional C 1s state at about 285.5 eV BE appears after deposition. This feature is denoted C1 in Fig. 4a. Fig. 4b shows the integrated intensities of the C1 state and the C 1s peak due to SiC. The peak related to SiC displays an exponential decay with exposure time. In contrast, the C1 state has a rather constant intensity up to 320 s of exposure time (about 20 \AA film thickness) after which it decreases slowly.

We propose that the C1 state in Fig. 4a is associated with methyl groups stemming from the ZTB precursor. This assignment is supported both by the C 1s BE and the intensity behavior for increasing film thickness. For ZTB-mediated ZrO_2 growth on Si(100) and Si(111) a C 1s state due to methyl groups was observed at 285.3 eV [23]. The intensity behavior of the C 1s peak due to methyl groups upon growth on Si(100) and Si(111) is found to be very similar to that shown in Fig. 4b. We argue that the point at which the methyl C 1s peak begins to decrease coincides with the point of interface completion [23]. From this follows that the methyl species is most likely correlated to the presence of Si surface atoms. The amount of surface Si atoms is expected to decrease once an extended ZrO_2 film forms. However, the decrease observed for films

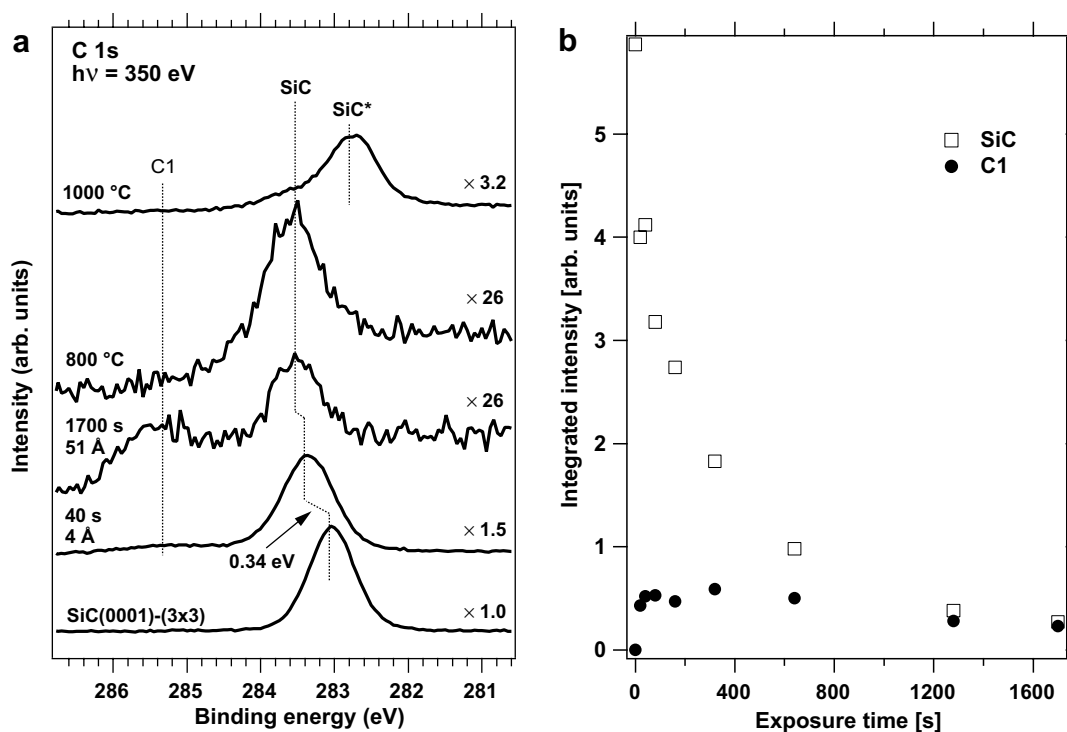


Fig. 4. (a) C 1s PES spectra for selected situations. The total energy resolution is set to 250 meV. Upon ZTB exposure the SiC bulk peak is shifted, most probably because of changes in the band bending. Small amounts of ZTB by-products are detected (C1 species). Upon annealing to 1000 °C the two C 1s components denoted SiC and SiC* can both be assigned to SiC bulk species. The C 1s high binding energy component (denoted SiC) is attributed to areas where the ZrO_2 overlayer remains. The C 1s low binding energy component (denoted SiC*) is attributed to areas where there is a metallic compound overlayer. (b) Integrated C 1s intensities for the SiC bulk component and the precursor induced C1 component, assigned to methyl groups.

thicker than 20 Å is slow. A feasible explanation for this is the tendency for intermixing of Si^{4+} with ZrO_2 as discussed in more detail below.

Moreover, for growth on Si(111) and Si(100) the interface region contains carbonaceous species which give rise to C 1s states having about 283–284 eV BE [23]. These are assigned to different hydrocarbon fragments with varying degree of coordination to Si [29,30]. Fig. 4a shows that the spectrum for a 51 Å thick film has some intensity between the bulk and C1 features. Thus, it cannot be excluded that several different carbon species are present also for growth on the Si-rich surface. However, the presence of the SiC bulk peak precludes a more detailed quantitative assessment of the ZTB related structures.

Selected Si 2p PES spectra measured using two different photon energies are presented in Figs. 5a and 5b. By comparing the more surface sensitive measurement using 130 eV photons (Fig. 5a) with the less surface sensitive measurement using 350 eV photons (Fig. 5b) it is possible to distinguish between bulk and surface species.

Each Si 2p spectrum for the Si-rich SiC(0001)-(3 × 3) surface can be described by four spin-orbit pairs [8]. These correspond to the SiC bulk species (SiC) and different species within the silicon overlayer (S1, S2 and S3). The fits were performed under the constraint that the width and relative position for each component are independent of photon energy. The lower resolution attained at higher photon energy (200 meV compared to 60 meV) is of no consequence as it is considerably smaller than the intrinsic width of the individual components (above 600 meV).

For each pair of Si 2p spectra we have employed a similar fitting procedure. Each spectrum is fitted using six spin-orbit pairs: One for the bulk (SiC), three originating from the silicon layer (SL1, SL2 and SL3) and two for oxidized silicon species (SiOX and Si^{4+}). In each spectrum the Gaussian FWHM broadening is 0.75 eV for the bulk component, 0.60 eV for each of the three silicon layer components and 1.10 eV for each of the two oxidized silicon components.

The identification of the bulk component from the surface sensitivity dependence is consistent with the C 1s spectra with regard to the BE shifts. The Si 2p and C 1s spectra measured using 350 eV photons are for each situation recorded in sequence and with the same experimental settings. Therefore, the relative binding energy shifts are very accurate. The Si 2p bulk peak is shifted +0.33 eV at 4 Å film thickness, nearly identical to the +0.34 eV found in the C 1s spectra. It has previously been reported that the BE:s of the core levels trace the shift of the valence band maximum for heterojunctions of semiconductors and insulators [31–33]. That the binding energies of the components attributed to SiC bulk species in the Si 2p and C 1s core level spectra respond approximately equally to changes in the band bending is thus a very reasonable result.

Fig. 5a clearly shows that there are states at lower BE:s than the bulk component also after the formation of an

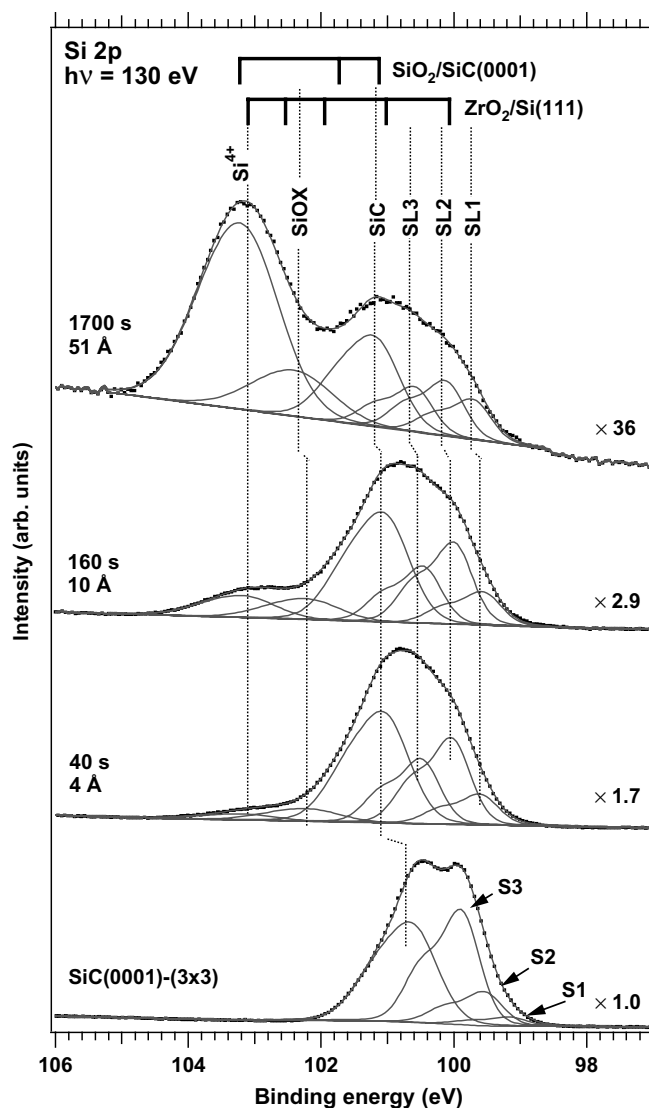


Fig. 5a. Selected Si 2p PES spectra measured using 130 eV photons from the film growth series. The total energy resolution is 60 meV. Labels are defined and discussed in the text. At the top relative binding energy positions from references are marked. The $\text{SiO}_2/\text{SiC}(0001)$ marker is set relative to the SiC bulk peak position and indicates from left to right the positions for Si^{4+} , Si^{1+} and SiC bulk [8]. The $\text{ZrO}_2/\text{Si}(111)$ marker is relative to the Si^{4+} position and indicates from left to right the positions for Si^{4+} , Si^{3+} , Si^{2+} , Si^{1+} and Si bulk [23].

oxide film. The spectral shapes of the low binding energy states are very similar from 4 Å to 51 Å. That is, fits can be performed in which the SL1, SL2 and SL3 states have approximately fixed relative intensities. The BE:s of the three components for the silicon layer after ZTB exposure are however not equivalent to the S1–S3 states of the clean reconstructed surface.

The most plausible interpretation is that the SL1–SL3 states are due to Si atoms originating from the Si adlayer. Previous results show that extensive oxidation using O_2 results in complete oxidation of the Si atoms in the Si adlayer [8]. A complete oxidation does apparently not occur upon reaction with the ZTB precursor at 400 °C. This can be due

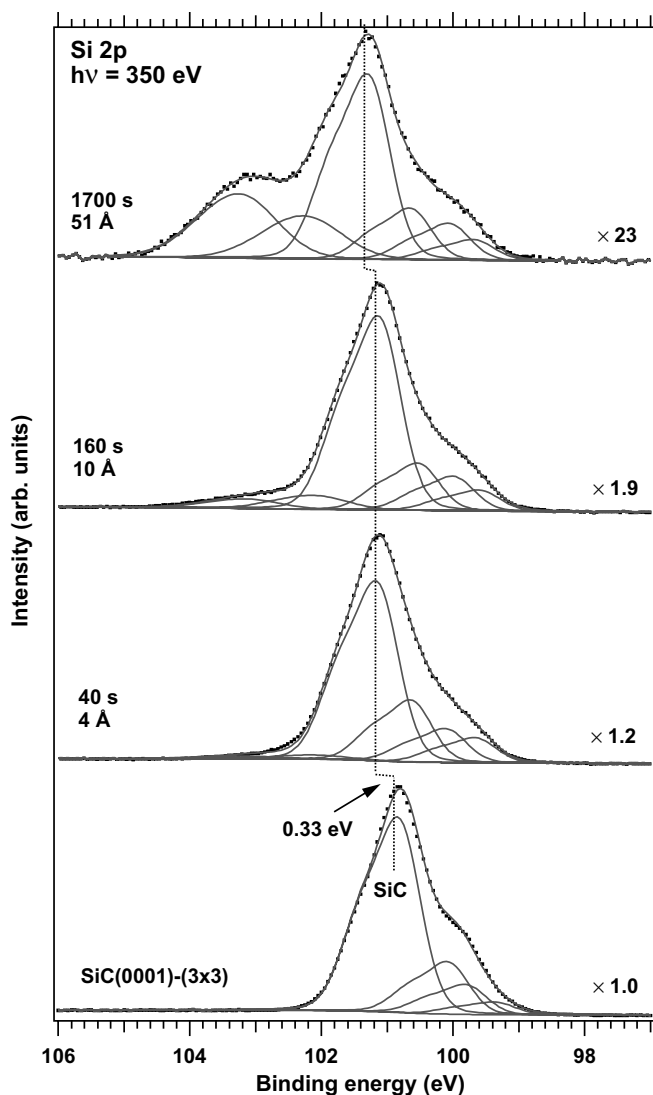


Fig. 5b. Comparably less surface sensitive Si 2p PES spectra for the same selected situations as in Fig. 6a. The spectra are measured using 350 eV photons. The total energy resolution is 200 meV.

to the fact that the oxidation with O_2 was accomplished using much larger doses (3000 L) as well as a higher temperature. However, it should be noted that the alkoxide precursors are strong oxidants when compared to O_2 . This has been demonstrated for titanium tetra isopropoxide on Si(111), where the tendency for Si oxidation far exceeds that of O_2 [26].

Another important aspect to take into account is the possibility for reaction of the Si atoms with hydrocarbon fragments, thereby interfering with the oxidation process. The study of ZTB-mediated ZrO_2 growth on Si(100) and Si(111) reveals the presence of Si 2p states shifted by -0.3 and $+0.3$ eV with respect to the bulk peak [23]. These states were assigned to result from Si interacting with hydrocarbons, carbon and hydrogen [23]. That states in the BE regime associated with the SL1–SL3 states appear due to reaction of Si adlayer atoms with hydrocarbon fragments is thus also a plausible explanation.

Turning next to the oxidized Si species a comparison to previous studies is valuable for the identification. At the top of Fig. 5a relative Si 2p_{3/2} BE positions from two reference systems, $SiO_2/SiC(0001)$ and $ZrO_2/Si(111)$, are indicated. The $SiO_2/SiC(0001)$ marker is set relative to the SiC bulk peak position and indicates from left to right the positions for Si^{4+} , Si^{1+} and SiC bulk [8]. The $ZrO_2/Si(111)$ marker is relative to the Si^{4+} position and indicates from left to right the positions for Si^{4+} , Si^3 , Si^{2+} , Si^{1+} and Si bulk [23].

The assignment of the Si^{4+} state is motivated by the binding energy [5,6]. Following the binding energy distribution of the oxidized silicon species previously found for growth on Si(111)-(7 × 7) [23] the state labeled SiOX may contain contributions from both Si^{2+} and Si^{3+} species, see Fig. 5a. The Si^{1+} component is possibly obscured by the SiC bulk component and/or a part of the SL3 component. Noteworthy is that the binding energy shift between the SL2 and Si^{4+} components is about 3 eV, which is similar to the binding energy shift found between the silicon bulk and Si^{4+} components for growth on Si(111)-(7 × 7) [23]. Thus, the SL2 feature may have a contribution from Si^0 species.

A summary of how the intensities of the components change as functions of film thickness is presented in Fig. 6a–c. The Si layer value is defined as the sum of the components attributed to the silicon layer (Si layer = SL1 + SL2 + SL3), and relative intensity refers to the intensity relative to the intensity of the SiC bulk component for each spectrum.

In Fig. 6a the relative intensities of the Si layer, SiOX and Si^{4+} components are plotted as functions of estimated film thickness. The spectra measured using 130 eV photons have been used. The relative intensity for the Si layer is approximately constant from 4 Å to 51 Å. The relative intensity of the component attributed to Si^{4+} species increases monotonically with increasing film thickness. In contrast, the relative intensity of the SiOX component increases up to an estimated film thickness of about 30 Å, and is thereafter approximately constant. The small decrease in relative intensity of the Si layer signal suggests that the part of the Si adlayer atoms that are not oxidized is substantial (at least 80%). However, it is clear that further studies, e.g. by performing angular scans, could prove to be most valuable in this respect.

The absolute intensities of the Si layer and Si^{4+} components are plotted as functions of estimated film thickness in Fig. 6b. Again, the spectra measured using 130 eV photons have been used. The absolute intensity of the Si layer component follows approximately an exponential attenuation function. The absolute intensity of the Si^{4+} component increases up to a film thickness of about 10 Å after which it is approximately constant.

In Fig. 6c we present measures of the relative surface sensitivity, calculated as the magnification of the relative intensity when changing the photon energy from 350 eV to 130 eV. The relative surface sensitivity of the bulk

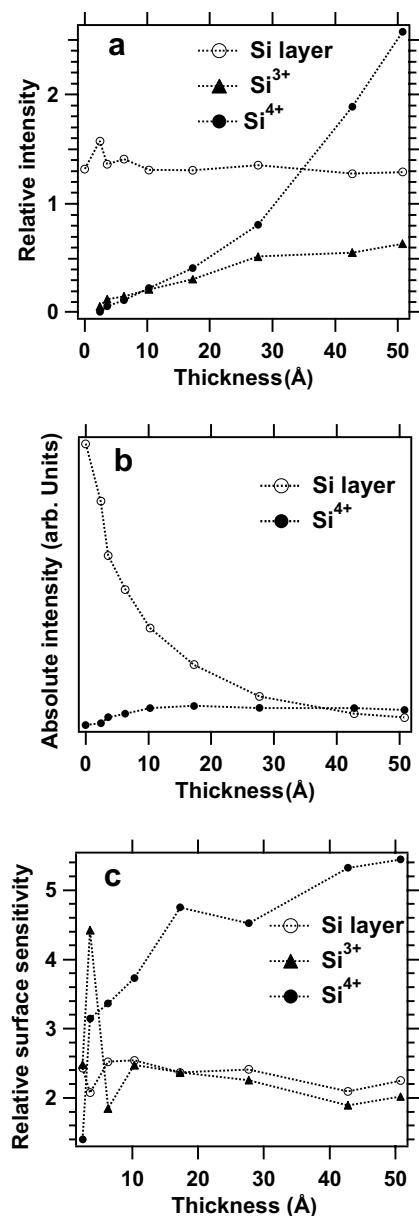


Fig. 6. Summary of results from the delineation of the Si 2p spectra recorded for the film growth experiments. (a) Relative intensities of the Si 2p components plotted as functions of film thickness. (b) Absolute intensities of the Si 2p components plotted as functions of film thickness. (c) Photon energy dependent changes of the relative intensities of the Si 2p components. These changes reflect the depth distribution of the different species.

species is thus by definition 1, and higher numbers corresponds to species closer to the surface. For the SiOX and Si⁴⁺ traces the numbers corresponding to low thicknesses are noisy due to uncertainties in determining the relatively small areas of the corresponding components.

The results in Fig. 6 indicate that the SiOX species has a similar depth position as the silicon layer and this position is fixed relative to the SiC bulk. The most straightforward interpretation is that the Si layer and SiOX species are situated at the interface between oxygen free and oxygen rich materials. The high relative surface sensitivity of the Si⁴⁺

Table 1

Summary of the analysis of the Si 2p spectra, giving the label, binding energy relative to the bulk SiC peak (BE, in eV), proposed assignment and preferential location of the various Si species within the ZrO₂/4H-SiC(0001) heterojunction

Label	Relative BE	Proposed assignment	Location
SL1	-1.50	Reconstructed Si adlayer (Si-H, Si)	Interface
SL2	-1.05	Reconstructed Si adlayer (Si-H, Si, Si-C)	Interface
SL3	-0.60	Reconstructed Si adlayer (Si-C, Si ¹⁺)	Interface
SiC	0.00		Bulk
SiOX	+1.12	Si ²⁺ , Si ³⁺	Interface
Si ⁴⁺	+2.03		Near surface

species indicates that there are Si⁴⁺ species in the near surface region, possibly intermixed with ZrO₂ (forming silicate). A similar behavior has previously been observed for HfO₂/SiO₂/Si(001) [34] and Al₂O₃/Si [35]. It was suggested in Ref. [34] that emission of Si species from the SiO₂/Si interface occurs in order to release the stress induced by oxidation. It can not be excluded that this also is the case for the ZrO₂/SiC(0001) system.

In summary, the analysis of the Si 2p spectra reveals that the reaction with the ZTB precursor is complex. This interface consist of a multitude of different Si species in contrast to that formed upon oxidation of Si(0001)-(3 × 3) by use of O₂. In Table 1, we summarize the discussion on the Si 2p data, providing proposed assignments and locations of the various Si species.

3.1.3. Band alignment

Studies of oxide growth on SiC are to a large extent motivated by the development of SiC electronic devices. Consequently, a discussion about the alignment of the valence band edges and the resulting band offsets are in place. We have recently demonstrated that a picture of the energy level arrangement can be obtained by combining PES and XAS [28].

Selected valence band PES spectra are presented in Fig. 7. The Si-rich SiC(0001)-(3 × 3) surface has a valence band spectrum similar to earlier published results [7,8]. It is observed that the feature between 1.0 and 1.5 eV, attributed to surface states for the reconstructed surface, has disappeared at 4 Å film thickness. The feature at around 3.1 eV consists of contributions from both the silicon layer and SiC bulk bands. It is attenuated upon film deposition, consistent with the results found from the Si 2p spectra. A shift towards higher BE is observed for this feature, analogous to the behavior of the Si 2p and C 1s bulk peaks. In the BE regime 5–10 eV new features appear, which grow with increasing exposure. These features are mainly associated with the valence band of ZrO₂ [28].

The film thickness dependent shifts of the VBES can be determined either from the shifts of the core levels or from valence difference spectra [28,31–33]. Using the former method, the VBE positions for SiC and ZrO₂ have been

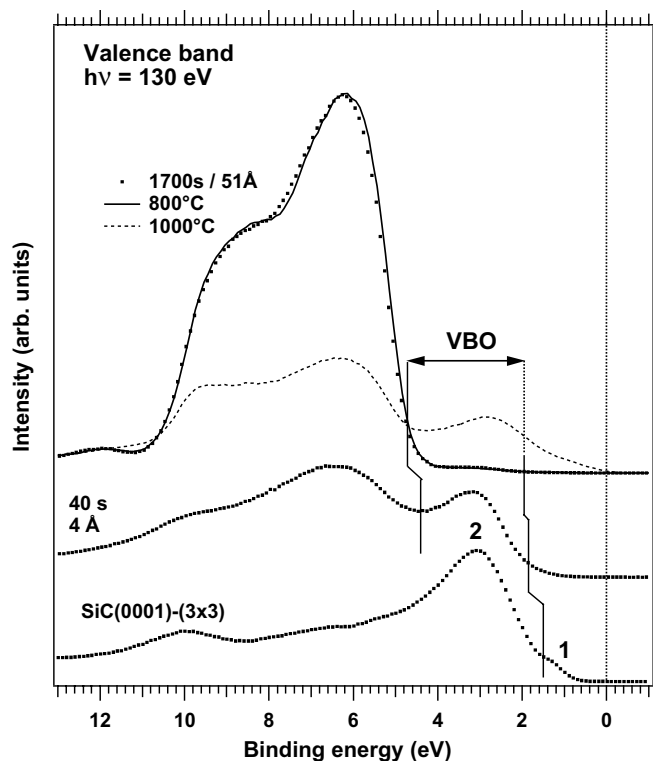


Fig. 7. Selected valence band spectra. Species 1 is attributed to surface states origination from the (3×3) surface reconstruction. Species 2 is related to the substrate and is attenuated upon deposition. The vertical solid lines indicate the locations of the SiC and ZrO_2 valence band edges and the resulting valence band offset (VBO). After subsequent annealing to 1000°C there are filled states all the way up to the Fermi level.

estimated and indicated by vertical solid lines in Fig. 7. It is observed that the valence band offset (VBO) increases with the film thickness, from 2.54 eV at 4 Å to 2.72 eV at 51 Å.

The location of the conduction band edge CBE can be estimated by adding band gap values from the literature (3.26 eV for 4H-SiC [36] and 5.40 eV for ZrO_2 [37]). Alternatively, the CBE position relative to the Fermi level can be obtained by comparing the O 1s PES spectrum to the corresponding O 1s XAS spectrum [28]. In Fig. 8, the O 1s PES and XAS spectra for the 51 Å thick film are put on a common energy scale. The values for the PES spectrum represent the BE relative to the Fermi level while the values for the XAS spectrum represent the absolute photon energy. By matching the low energy side of the PES spectrum to the XAS threshold, an estimate of the CBE relative to the Fermi level is obtained. In the case of the 51 Å thick ZrO_2 film the CBE is located 1.05 eV above the Fermi level. This gives a band gap of 5.40 eV when adding the VBE position found in the valence PES spectrum, in excellent agreement with Ref. [37].

In Fig. 9 the band alignment for 4 Å and 51 Å thick films are presented. With respect to the prospect of using this system in MOSFET applications the band alignment is too asymmetric. In order to be feasible the ZrO_2 band edges must be shifted downwards in BE by 1.5–2 eV relative to the SiC band edges [22,33]. It can be speculated that

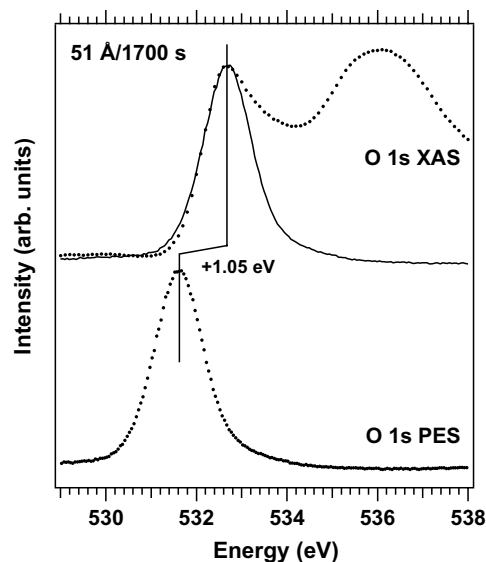


Fig. 8. O 1s PES and XAS spectra for the 51 Å thick ZrO_2 film deposited on the Si-rich SiC(0001)- (3×3) surface. The energy values for the PES spectrum are relative to the Fermi level, whereas the energy values for the XAS spectrum correspond to the absolute photon energy. The energy needed to match the low energy side of the PES spectrum to the XAS threshold gives an estimate of the location of the conduction band edge relative to the Fermi level [28].

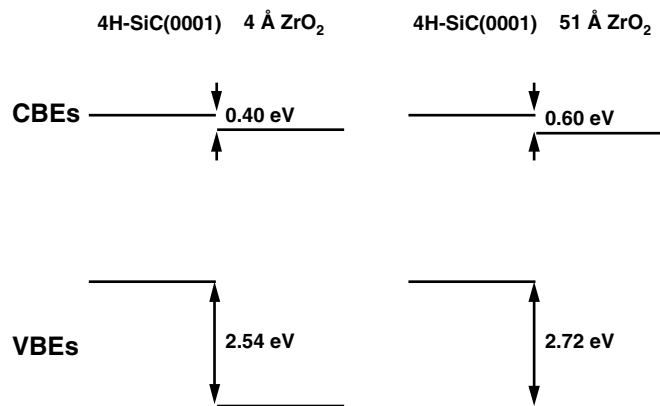


Fig. 9. Band alignment of the $\text{ZrO}_2/4\text{H-SiC}(0001)$ system formed by ZrO_2 growth on the Si-rich SiC(0001)- (3×3) system. The locations of the valence band edges (VBEs) are determined from valence and core level PES data. The location of the conduction band edges (CBEs) are estimated from literature values of the band gaps, O 1s PES and O 1s XAS spectra.

the procedure adopted here, i.e. deposition on the Si-rich SiC(0001)- (3×3) surface, is not optimal in this respect.

3.2. Thermal stability

3.2.1. Annealing to 800°C

The estimated overlayer thickness decreases by a few percent upon annealing the film grown at $400\text{--}800^\circ\text{C}$. No observable changes appear in the Zr 3d and O 1s signals. However, the C1 species has disappeared in the corresponding C 1s signal, as can be seen in Fig. 4a. That is, the

surface methyl groups have vanished, most probably under the formation of desorbing species.

The Si $2p_{3/2}$ lines measured using 130 eV photons and 350 eV photons are presented in Figs. 10a and 10b, respectively. Only the Si $2p_{3/2}$ line is presented to better illustrate the changes upon heating. The spectra are obtained after subtraction of a calculated background followed by removal of a calculated Si $2p_{1/2}$ line. After annealing to 800 °C the sum of the relative intensities of the components on the low binding energy side of the bulk component has decreased. The components on the low binding energy side of the bulk component are furthermore more separated in BE. It is reasonable that the extension of states towards lower BE:s signatures the formation a new type of silicon species, possibly involving bonds to zirconium, cf. below.

It is observed that the relative intensities of the components attributed to oxidized silicon species increase. The component SiOX representing intermediate oxidation states has both increased in relative intensity and shifted towards the bulk peak. This is a possible indication of oxidation of SiC. To clarify, formation of Si^{1+} is expected at a binding energy shifted +0.6 eV from the bulk peak [8]. The position found for SiOX is +0.7 eV from the bulk peak.

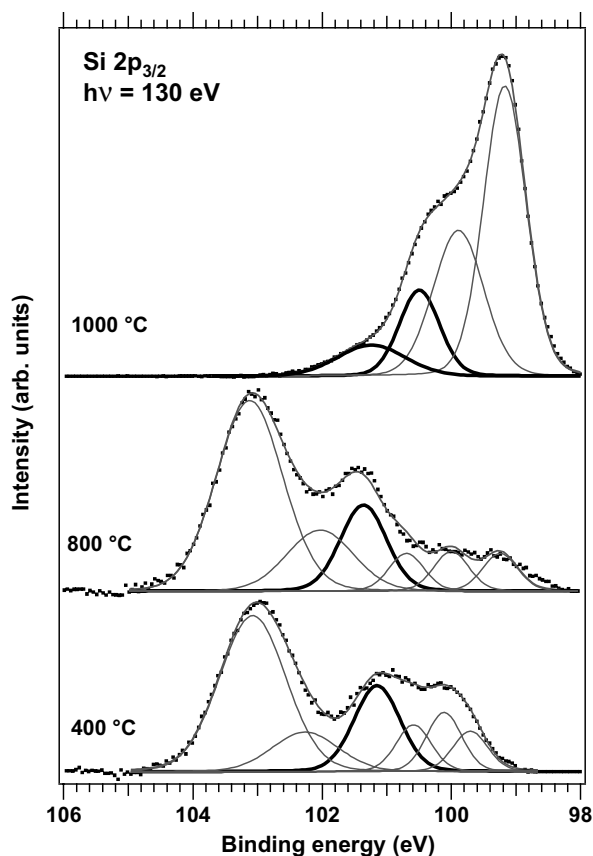


Fig. 10a. Surface sensitive measurements for the thermal stability experiments. The presented Si $2p$ spectra are those obtained after background subtraction and Si $2p_{1/2}$ stripping. The total energy resolution is 60 meV. Labels are defined and discussed in the text.

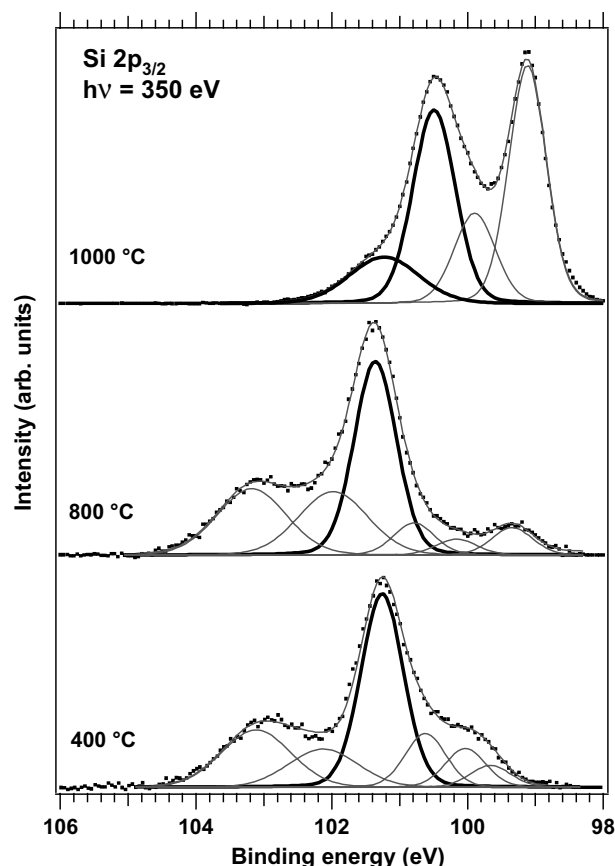


Fig. 10b. Less surface sensitive measurements for the same selected situations as in Fig. 9a. The presented Si $2p$ spectra are those obtained after background subtraction and Si $2p_{1/2}$ stripping. The total energy resolution is 200 meV.

Very small changes in the valence spectrum are observed. The feature around 3.1 eV becomes slightly less pronounced, consistent with the changes in the low BE Si $2p$ components associated with the silicon layer.

In summary, annealing to 800 °C does not lead to any appreciable changes in the ZrO_2 film. However, changes are observed that signals the beginning of interface decomposition.

3.2.2. Annealing to 1000 °C

Upon subsequent annealing to 1000 °C the estimated average thickness is reduced to around 20 Å, i.e. by more than 50%. Fig. 3 shows that the Zr 3d spectrum is dramatically different compared to that of the as grown film. A new additional component at about 5 eV lower BE than the Zr^{4+} component has appeared. From the BE position and the asymmetric line shape [38] this component is attributed to zirconium atoms in a compound having metallic properties. Noteworthy is that the relative area between the two zirconium species does not change dramatically when changing the surface sensitivity of the measurement, as can be seen in Fig. 3. This indicates that the surface region is heterogeneous, i.e. the two Zr species stem from laterally different parts.

The valence spectra change dramatically upon annealing to 1000 °C as seen in Fig. 8. The most apparent effect is the decrease of the intensity of the ZrO₂ valence band. However, the most important finding is that there are filled states all the way up to the Fermi level. This supports the notion of the formation of a metallic compound.

The absolute intensity of the O 1s signal (spectrum not shown) decreases upon annealing to 1000 °C but the shape of the spectrum is retained. In line with the interpretation of the Zr 3d spectrum the O 1s signal is mainly attributed to remaining ZrO₂. The O 1s XAS spectrum (not shown) reveals that the tetragonal structure is maintained.

The C 1s spectrum is shown in Fig. 4a. The signal increases and a reasonable fit can be performed using two components, each having the same width as found for the bulk species for the Si-rich SiC(0001)-(3 × 3) surface. This procedure results in a binding energy separation of 0.8 eV and an intensity ratio of 0.25 between the two components. The two C 1s components denoted SiC and SiC* in can both be assigned to SiC bulk species. This is consistent with a laterally heterogeneous film as inferred from the Zr 3d spectra. The C 1s high binding energy component (denoted SiC) is attributed to areas where the ZrO₂ overlayer remains. This is motivated by the similarity in binding energy position compared to that of the as grown film. The C 1s low binding energy component (denoted SiC*) is attributed to areas where there is a metallic compound overlayer.

The BE for the C 1s peak labeled SiC* is 0.3 eV lower than that of SiC bulk for the Si-rich SiC(0001)-(3 × 3) surface. Thus, the core level shifts of the bulk component imposed by ZrO₂ and metallic silicide are in opposite directions. In a simple band-bending picture [39] this behavior is possible if the two different overlaying materials have significantly different work functions or laterally locally different interface states. Shifts in opposite directions can also in principle be rationalized in terms of different screening properties but the effect of screening is expected to be more local in nature [40].

The Si 2p spectra change dramatically in shape upon annealing to 1000 °C and the absolute integrated intensity increases. At least four components are needed to delineate the spectra. The components presented in Figs. 10a and 10b are symmetric but most likely there are silicon species in an environment having metallic properties. However, introduction of reasonable asymmetries [38] in different combinations have limited effects on the resulting relative intensities and binding energy positions.

By comparing the more surface sensitive measurements with the less surface sensitive measurements it is possible to distinguish between bulk and surface species. The two components on the high binding energy side should be attributed to SiC bulk. In the Si 2p spectrum measured at 350 eV photon energy the intensity ratio and binding energy difference between the two components attributed to SiC bulk are similar to those found for the corresponding

C 1s spectrum. The two components on the low binding energy side are surface species. Based on the observation of Zr 3d states in a metallic environment, the state of 99.1 eV BE is tentatively assigned to compounds of the type ZrSi_x. The state labeled Si in Fig. 10a has a BE of 100.0 eV, which is very similar to that of the most abundant Si species for the Si-rich SiC(0001)-(3 × 3) surface. This suggests that it may be associated with Si aggregates on the surface.

The results thus show that the ZrO₂ film decomposes upon annealing to 1000 °C. A heterogeneous layer is formed that can be subdivided laterally in regions with remnants of the t-ZrO₂ film, metallic Zr silicide and, possibly, areas with a Si aggregates. The thermal stability under vacuum is similar to that observed for ultrathin ZrO₂ films on Si(100) [41,42]. It has been argued that the ZrO₂/Si(100) structure is stable up to 800 °C and that a reaction leading to the formation of zirconium silicide occurs around 900 °C [41,42]. Regarding the stability at 800 °C it should be noted that the quality of the reported data on annealed ZrO₂/Si(100) makes an observation of the subtler details found in the present study very difficult. It was furthermore shown that formation of ZrSi₂ is most likely, as it is the most thermodynamically stable metal silicide for the ZrO₂/Si system [41,42]. However, since the substrate in the present case is SiC there may be additional possibilities. For instance, compounds containing carbon atoms must be considered.

4. Conclusions

The growth and thermal stability of ultrathin ZrO₂ films on the Si-rich SiC(0001)-(3 × 3) surface have been explored using photoelectron spectroscopy (PES) and X-ray absorption spectroscopy (XAS). The films were grown *in situ* by chemical vapor deposition using the zirconium tetra *tert*-butoxide (ZTB) precursor. During exposure to ZTB the samples were heated to 400 °C, which results in growth of tetragonal ZrO₂. An interface is formed between the ZrO₂ film and the SiC substrate. The interface contains Si in various suboxidation states. Confined within the interface are also Si species formed by reactions with hydrocarbon fragments of the ZTB molecule. Si in a 4+ oxidation state is detected in the near surface region. This shows that intermixing of SiO₂ and ZrO₂ occurs, possibly under the formation of silicate. The SiC–ZrO₂ band alignment was discussed with the aid of valence PES and O 1s XAS spectra. It is found that the as-prepared system does not fulfill the band alignment required for a MOSFET device. Subsequent annealing of a deposited film was performed in order to study the thermal stability of the system. Annealing to 800 °C does not lead to decomposition of the tetragonal ZrO₂ (t-ZrO₂) but changes are observed within the interface region. After annealing to 1000 °C a heterogeneous layer has formed. The decomposition of the film leads to regions with t-ZrO₂ remnants, metallic Zr silicide and Si aggregates.

Acknowledgements

The authors acknowledge the assistance from the MAX-lab staff and the financial support from the Swedish Science Council (VR) and the Göran Gustafsson Foundation.

References

- [1] L.A. Lipkin, J.W. Palmour, *J. Electron. Mater.* 25 (1996) 909.
- [2] V.R. Vathulya, D.N. Wang, M.H. White, *Appl. Phys. Lett.* 73 (1998) 2161;
V.V. Afanas'ev, A. Stesmans, M. Bassler, G. Pensl, M.J. Schulz, C.I. Harris, *Appl. Phys. Lett.* 68 (1996) 2141.
- [3] V.V. Afanas'ev, A. Stesmans, *Appl. Phys. Lett.* 69 (1996) 2252;
V.V. Afanas'ev, A. Stesmans, M. Bassler, G. Pensl, M.J. Schulz, C.I. Harris, *J. Appl. Phys.* 85 (1999) 8292.
- [4] F. Amy, H. Enriquez, P. Soukiassian, P.-F. Storino, Y.J. Chabal, A.J. Mayne, G. Dujardin, Y.K. Hwu, C. Brylinski, *Phys. Rev. Lett.* 86 (2001) 4342.
- [5] Y. Hoshino, T. Nishimura, T. Yoneda, K. Ogawa, H. Namba, Y. Kido, *Surf. Sci.* 505 (2002) 234.
- [6] F. Amy, P. Soukiassian, Y.K. Hwu, C. Brylinski, *Phys. Rev. B* 65 (2002) 165323.
- [7] C. Virojanadara, L.I. Johansson, *J. Phys. C* 16 (2004) S1783.
- [8] C. Virojanadara, L.I. Johansson, *Phys. Rev. B* 71 (2005) 195335.
- [9] K.Y. Gao, Th. Seyller, L. Ley, F. Ciobanu, G. Pensi, A. Tadich, J.D. Riley, R.G.C. Leckey, *Appl. Phys. Lett.* 83 (2003) 1830.
- [10] D.R. Clarke, S.R. Phillpot, *Mater. Today* 8 (2005) 22.
- [11] G.D. Wilk, R.M. Wallace, J.M. Anthony, *J. Appl. Phys.* 89 (2001) 5243.
- [12] J.P. Chang, Y.-S. Lin, S. Berger, A. Kepten, R. Bloom, S. Levy, *J. Vac. Sci. Technol. B* 19 (2001) 2137.
- [13] B.-O. Cho, J.P. Chang, *Appl. Phys. Lett.* 93 (2003) 745.
- [14] W.Y. Lee, H. Li, Y.-F. Su, *Mater. Sci. Forum* 426–432 (2003) 137.
- [15] K. Shibata, T. Oi, A. Otsuka, H. Sumitomo, K. Oshihara, Y. Teraoka, W. Ueda, *J. Ceram. Soc. Jpn.* 111 (2003) 852.
- [16] F. Amy, P. Soukiassian, Y.K. Hwu, C. Brylinski, *Appl. Phys. Lett.* 75 (1999) 3360.
- [17] F. Amy, P. Soukiassian, Y.K. Hwu, C. Brylinski, *Surf. Sci. Lett.* 464 (2000) 691.
- [18] F.S. Tautz, S. Sloboshanin, U. Starke, J.A. Schaefer, *Surf. Sci.* 470 (2000) L25.
- [19] K. Reuter, J. Bernhardt, H. Wedler, J. Schardt, U. Starke, K. Heinz, *Phys. Rev. Lett.* 79 (1997) 4818.
- [20] U. Starke, J. Schardt, J. Bernhardt, M. Franke, K. Reuter, H. Wedler, K. Heinz, J. Furthmüller, P. Käckell, F. Bechstedt, *Phys. Rev. Lett.* 80 (1999) 758.
- [21] J.N. Andersen, O. Björneholm, A. Sandell, R. Nyholm, J. Forsell, L. Thånell, A. Nilsson, N. Mårtensson, *Synchrotron Radiat. News* 4 (1991) 15.
- [22] R. Puttenkovikalam, E.A. Carter, J.P. Chang, *Phys. Rev. B* 69 (2004) 155329.
- [23] P.G. Karlsson, J.H. Richter, J. Blomquist, P. Uvdal, T.M. Grehk, A. Sandell, *Surf. Sci.* 601 (2007) 1008.
- [24] P.W. Peacock, J. Robertson, *Phys. Rev. Lett.* 92 (2004) 057601.
- [25] An approximately linear relationship between the core level binding energy and oxidation state is commonly observed for semiconductors and insulators [F.J. Himpsel, F.R. McFeely, A. Taleb-Ibrahimi, J.A. Yarmoff, G. Holling, *Phys. Rev. B* 38 (1988) 6084]. The 3d core level shift between Zr⁴⁺ and metallic Zr silicide is 4.9 eV. From this follows that the core level shift between Zr⁴⁺ and Zr³⁺ should amount to about 1.2 eV.
- [26] A. Sandell, M.P. Andersson, M.K.-J. Johansson, P.G. Karlsson, Y. Alfredsson, J. Schnadt, H. Siegbahn, P. Uvdal, *Surf. Sci.* 530 (2003) 63.
- [27] K. Sakamoto, H.M. Zhang, R.I.G. Uhrberg, *Phys. Rev. B* 68 (2003) 075302.
- [28] A. Sandell, P.G. Karlsson, J.H. Richter, J. Blomquist, P. Uvdal, T.M. Grehk, *Appl. Phys. Lett.* 88 (2006) 132905.
- [29] A. Fink, W. Widdra, W. Wurth, C. Keller, M. Stichler, A. Achleitner, G. Comelli, S. Lizzit, A. Baraldi, D. Menzel, *Phys. Rev. B* 64 (2001) 045308.
- [30] H. Liu, R. Hamers, *Surf. Sci.* 416 (1998) 354.
- [31] E.A. Kraut, R.W. Grant, J.R. Waldrop, S.P. Kowalczyk, *Phys. Rev. Lett.* 44 (1980) 1620.
- [32] E.A. Kraut, R.W. Grant, J.R. Waldrop, S.P. Kowalczyk, *Phys. Rev. B* 28 (1983) 1965.
- [33] R. Puthenkovikalam, J.P. Chang, *Appl. Phys. Lett.* 84 (2004) 1353.
- [34] K.Y. Gao, F. Speck, K. Emtsev, Th. Seyller, L. Ley, M. Oswald, W. Hansch, *Phys. Stat. Sol. A* 203 (2006) 2194.
- [35] Z. Ming, K. Nakajima, M. Suzuki, K. Kimura, M. Uematsu, K. Torii, S. Kamiyama, Y. Nara, K. Yamada, *Appl. Phys. Lett.* 88 (2006) 153516.
- [36] V.V. Afanas'ev, M. Bassler, G. Pensl, M.J. Schulz, E. Stein von Kamienski, *J. Appl. Phys.* 101 (2007) 034108.
- [37] V.V. Afanas'ev, F. Ciobanu, S. Dimitrijević, G. Pensl, A. Stesmans, *J. Phys.: Condens. Matter.* 16 (2004) S1839.
- [38] S. Doniach, M. Sunjic, *J. Phys. C* 3 (1970) 285.
- [39] C. Kittel, *Introduction to solid state physics*, 1986. ISBN: 0-471-87474-4;
S.M. Sze, *Semiconductor devices, physics and technology*, 2001. ISBN: 0-471-33372-7.
- [40] T.C. Chiang, G. Kaindl, T. Mandel, *Phys. Rev. B* 33 (1986) 695.
- [41] T.S. Jeon, J.M. White, D.L. Kwong, *Appl. Phys. Lett.* 78 (2001) 368.
- [42] J.P. Chang, Y.-S. Lin, *Appl. Phys. Lett.* 79 (2001) 3824.